

## Optical parametric oscillator far below threshold: Experiment versus theory

Y. J. Lu and Z. Y. Ou

*Department of Physics, Indiana University–Purdue University Indianapolis, 402 N. Blackford Street, Indianapolis, Indiana 46202*

(Received 9 February 2000; published 8 August 2000)

The theory of the optical parametric oscillator is examined and compared to the experiment in the regime of far below threshold. It is found that the output state has no difference from spontaneous parametric down-conversion except that the bandwidth of down-conversion is reduced to that of the resonator and the conversion rate is enhanced by cavity resonance. The reduction of the bandwidth of the down-converted fields makes it possible for a direct measurement of the time interval distribution between two down-converted photons. The observed distributions are well explained by the theory. Such a narrow-band two-photon source will find wide applications in quantum information processing.

PACS number(s): 42.50.Dv, 03.65.Bz, 42.25.Hz

### I. INTRODUCTION

Because of its ability to produce a two-photon state that is highly entangled in many degrees of freedom, the process of spontaneous parametric frequency down-conversion has been thoroughly studied in recent years ever since the pioneering work by Burnham and Weinberg [1] and the more recent work by Friberg *et al.* [2] and Hong and Mandel [3]. It has been widely applied to the demonstration of quantum nonlocality [4,5] and quantum interference [6–9], and more recently to quantum information processing [10–12]. The technique of photon counting is applied in these experiments to utilize the strong correlation between photons. The down-converted light is produced in a single-pass fashion with weak interaction to preserve the two-photon nature of the state. Concurrent with the study of photon correlation is another entirely different approach that utilizes the parametric down-conversion process for the generation of a squeezed state of light with reduced quantum noise [13]. A complete different detection scheme based on homodyne and/or heterodyne detection is used in this approach to characterize quantum noise in amplitudes. Because of the strong nonlinearity required for large noise reduction, the optical cavity is often used to form an optical parametric oscillator (OPO) so that the down-converted fields pass the nonlinear medium numerous times and the device is operated near or above threshold. This leads to a different formalism in the theoretical treatment. For the single-pass case, the interaction is weak and the perturbation approach is used, resulting in a correlated two-photon state while for the OPO, an exact solution of the equation of motion has to be obtained. Superficially, there seems to be no connection between these two approaches, which investigate two totally different aspects of the parametric down-conversion process, i.e., photon correlation (particle aspect) and amplitude correlation (wave aspects). But they are essentially based on one common trait of the process, that is, the quantum correlation between the two conjugate fields. Shapiro and Sun made a successful attempt to establish the link between these two approaches [14].

Recently, there has been renewed interest in the interference between independent sources, mainly for the applications in quantum information processing [10,11]. In these applications, two or more independent fields from the para-

metric down-conversion process are mixed to create quantum entanglement among them. Quantum entanglement is an essential ingredient in quantum information science. Historically, the first experiment on the interference between two independent sources was performed by Magyar and Mandel in 1963 [15]. Since classical sources were used for the optical fields in that experiment, it does not have any practical application in quantum information science other than serving as a proof of principle. Later on, it was shown that the bandwidth of the independent sources must be much smaller than that of the detectors in order to achieve high visibility in the interference between independent stationary fields of any kind [16]. On the one hand, most of the applications of the single-pass spontaneous parametric down-conversion process rely on the extremely short correlation time ( $\approx 1$  ps) between the two photons. On the other hand, due to an extra degree of freedom for the down-conversion process (two frequency components are produced), the only limitation on the bandwidth comes from the phase matching condition, which sets a loose constraint on the frequencies of down-converted photons and gives rise to a wide bandwidth of a typical value of  $10^{13}$  Hz. This is much wider than the response bandwidth of the fastest photodetector available (typically  $10^{10}$  Hz). Thus single-pass spontaneous parametric down-conversion cannot be used in quantum interference between independent sources without modification. In order to reduce the bandwidth, we may either use a narrow band-pass filter [17] or a small pinhole [18]. For the reduction of the bandwidth to the sub-GHz level (to match the bandwidth of the detectors), both methods, when applied, will significantly decrease the flux of the photon pairs because the photon number is proportional to the bandwidth (or number of modes) owing to the spontaneous nature of the process.

It should be mentioned that the bandwidth requirement discussed above is strictly for cw (stationary) fields. So in tackling the bandwidth problem, Rarity *et al.* and Zukowski *et al.* [19] proposed a scheme that utilizes a pulsed (nonstationary) field to provide a well-defined temporal mode for interference. The variations of the proposed schemes were successfully implemented, but rather low visibility was observed in these demonstrations [10,11]. More detailed analysis [20] shows that the low visibility is due to intrinsic improper temporal mode matching for pulsed fields and that

narrow band-pass (passive) filters are needed to improve the mode matching for high visibility. But as we discussed earlier, the consequence of passive filtering is a substantial reduction of the signal level in these experiments.

The signal reduction problem can be solved by combining the two approaches in the study of the parametric down-conversion process mentioned in the beginning. It is known that OPO produces narrow-band fields due to the resonance condition embedded in optical cavity. That is why homodyne and/or heterodyne detection is possible even though such a detection scheme involves interference between independent fields of quantum source and strong local oscillator (coherent field). However, for the generation of the narrow-band two-photon state, the device cannot be operated near threshold because the stimulated process will overwhelm the spontaneous process and produce a photon state with a higher number (more than two) besides the two-photon state. To reduce the stimulated process to a negligible level, the device has to be operated far below threshold. This regime of operation of OPO has never been explored before. The effect of cavity on the spontaneous two-photon process is quite similar to the cavity QED effect on atomic emission [21,22]. The cavity will enhance some of the down-conversion modes selected by the cavity resonance and in the meanwhile inhibit other nonresonant modes. So contrary to the passive filtering scheme with the filter placed after the light is generated, this scheme of active filtering with the source inside the filter will reduce the bandwidth without sacrificing the signal level.

In this paper we will discuss a specific scheme of active filtering for reducing the bandwidth of the down-conversion. Quite different from the single-pass case, light passes through the nonlinear medium many times, thus equivalently lengthening the interaction distance. We will demonstrate that by making both down-conversion components resonant with the cavity (double resonance), the interaction length is effectively increased by  $\mathcal{F}$  times with  $\mathcal{F}$  being the finesse of the cavity or equivalently the number of round trips in the cavity for the photons before they are coupled out. The enhancement can be thought of as the result from a constructive two-photon interference. To ensure production of only a two-photon state, the pump power has to be carefully controlled to operate at a relatively low level so that the stimulated process can be neglected. The outline of the paper is as follows: We will start in Sec. II with a general theory of an optical parametric oscillator below threshold. Then in Sec. III we discuss the mode structure for the device and the method for single-mode operation. We will study the time correlation between the two photons generated in OPO for both multimode and single-mode operation in Sec. IV. Section V will be devoted to experimental verification of the theoretical results in Secs. II–IV. We conclude the paper in Section VI. Preliminary results in this paper have been published in Ref. [23].

## II. GENERAL THEORY OF OPO

The optical parametric oscillator as the first nonlinear optical device was originally constructed as a tunable source for spectroscopic application [24] and is usually operated far

above threshold as a classical coherent source. It was later shown that when operated under threshold, OPO becomes a quantum device and can generate squeezed states of light [25,26], and when operated above but near threshold it produces correlated twin-photon fields [27]. For large quantum effects, the device has to be operated close to threshold. So far the quantum theory of OPO has been tested well against experiment in these regimes. However, for the regime of far below threshold, there has been neither experimental nor theoretical investigations. In this regime, we should expect stimulated emission to be negligible compared to spontaneous emission and the result is a simple two-photon state similar to the single-pass case. A number of versions of the quantum theory of OPO exist with an emphasis on the regime close to but under threshold [26,28]. A close examination leads us to believe that they should apply equally well to the regime far below threshold. As shown by Collett and Gardiner [26], the output operator of a degenerate OPO on resonance is related to the input as follows [Eq. (46) of Ref. [26]]:

$$a_{out}(\omega_0 + \omega) = G_1(\omega)a_{in}(\omega_0 + \omega) + g_1(\omega)a_{in}^\dagger(\omega_0 - \omega) + G_2(\omega)b_{in}(\omega_0 + \omega) + g_2(\omega)b_{in}^\dagger(\omega_0 - \omega), \quad (1)$$

with

$$G_1(\omega) = \frac{\gamma_1 - \gamma_2 + 2i\omega}{\gamma_1 + \gamma_2 - 2i\omega}, \quad g_1(\omega) = \frac{4\epsilon\gamma_1}{(\gamma_1 + \gamma_2 - 2i\omega)^2},$$

$$G_2(\omega) = \frac{2\sqrt{\gamma_1\gamma_2}}{\gamma_1 + \gamma_2 - 2i\omega}, \quad g_2(\omega) = \frac{4\epsilon\sqrt{\gamma_1\gamma_2}}{(\gamma_1 + \gamma_2 - 2i\omega)^2}. \quad (2)$$

Here  $\epsilon$  is the single-pass parametric amplitude gain and is proportional to the pump amplitude and the nonlinear coefficient. In Eq. (2) we have dropped the  $|\epsilon|^2$  term in the denominator because the OPO is operated far below threshold so that  $|\epsilon| \ll \gamma_1, \gamma_2$ .  $\omega_0$  is the degenerate frequency of the OPO.  $\hat{b}_{in}$  represents the unwanted vacuum mode coupled-in due to losses in the system.  $\gamma_1, \gamma_2$  are the coupling constants (decay constants) for  $\hat{a}_{in}$  and  $\hat{b}_{in}$ , respectively.

First, let us look at the enhancement effect in the down-conversion due to resonance. For this, we calculate from Eq. (1) the spectrum of the field  $S(\omega)$  defined by

$$\langle a_{out}^\dagger(\omega_0 + \omega)a_{out}(\omega_0 + \omega') \rangle \equiv S(\omega)\delta(\omega - \omega'). \quad (3)$$

The result is

$$S(\omega) = |g_1(\omega)|^2 + |g_2(\omega)|^2 = \frac{16|\epsilon|^2\gamma_1(\gamma_1 + \gamma_2)}{[(\gamma_1 + \gamma_2)^2 + 4\omega^2]^2}. \quad (4)$$

The rate of down-conversion can be calculated as

$$R_{cavity} = \langle E_{out}^{(-)}(t)E_{out}^{(+)}(t) \rangle = \frac{1}{2\pi} \int d\omega S(\omega), \quad (5)$$

where

$$\hat{E}^{(+)}(t) = [\hat{E}^{(-)}(t)]^\dagger = \frac{1}{\sqrt{2\pi}} \int d\omega \hat{a}(\omega) e^{-i\omega t}. \quad (6)$$

From Eq. (4), we have

$$R_{cavity} = \frac{1}{2\pi} \int_{-\infty}^{\infty} d\omega \frac{16|\epsilon|^2 \gamma_1 (\gamma_1 + \gamma_2)}{[(\gamma_1 + \gamma_2)^2 + 4\omega^2]^2} = |r|^2 \mathcal{F}^2 / \pi \Delta t \mathcal{F}_0, \quad (7)$$

where  $r \equiv \epsilon \Delta t$  is the single-pass gain parameter with  $\Delta t$  as the round-trip time, and  $\mathcal{F} \equiv 2\pi / (\gamma_1 + \gamma_2) \Delta t = 2\pi / \Delta t \Delta \omega_{opo}$  is the finesse of the cavity (which is of the order of the number of bounces of light before it leaves the cavity) and can be measured directly. Here  $\Delta \omega_{opo} = \gamma_1 + \gamma_2$  corresponds to the bandwidth of the OPO cavity.  $\mathcal{F}_0 \equiv 2\pi / \gamma_1 \Delta t$  is the same quantity without the loss ( $\gamma_2 = 0$ ). To find the enhancement factor, we need the signal rate without the cavity. In the single-pass case, we simply have  $g_1(\omega) = r \eta(\omega)$  and  $g_2 = 0$ . Here  $\eta(\omega)$  is the gain spectrum of single-pass spontaneous down-conversion determined by a phase-matching condition with normalization  $\eta(0) = 1$ . In the experiment, we usually have an interference filter (IF) in front of the detector. The bandwidth  $\Delta \omega_{IF}$  of IF is normally smaller than that of down-conversion so that  $\eta(\omega) \approx 1$  for  $\omega$  within  $\Delta \omega_{IF}$  and is zero for  $\omega$  outside  $\Delta \omega_{IF}$ . Hence, the signal rate without the cavity is

$$R_{singlepass} = |r|^2 \Delta \omega_{IF} / 2\pi, \quad (8)$$

and the average enhancement factor per mode is

$$B \equiv \frac{R_{resonance} / \Delta \omega_{opo}}{R_{singlepass} / \Delta \omega_{IF}} = \mathcal{F}^3 / \pi \mathcal{F}_0, \quad (9)$$

or roughly the square of the number of bounces of light before it leaves the cavity, consistent with the two-photon nature of parametric down-conversion. The square law is a result of two-photon constructive interference. The loss of the system will reduce the effect by a factor of  $\mathcal{F} / \mathcal{F}_0$ .

### III. MODE STRUCTURE

It is known that the optical cavity allows simultaneous resonance of a number of frequencies (longitudinal modes of the cavity). The double resonance condition for parametric down-conversion will reduce the number. But depending on whether it is a type-I or -II down-conversion process, we may still have more than one frequency mode simultaneously on resonance in the cavity. Even for a single mode of the cavity, the field still has multifrequency components with a bandwidth of  $\Delta \omega_{opo}$ .

#### A. Type-I down-conversion

The two highly correlated fields have the same polarization in type-I parametric down-conversion. For studying the interference effect, it is preferable to make them equal in frequency. This corresponds to degenerate parametric down-conversion. The resonance condition requires that

$$\omega_0 = \frac{2\pi N_0 c}{l + n(\omega_0)d} \quad \text{or} \quad [l + n(\omega_0)d] \omega_0 = 2\pi N_0 c, \quad (10)$$

for the degenerate frequency  $\omega_0$ . Here  $N_0$  is some integer,  $d$  is the length of the nonlinear crystal providing parametric interaction,  $n(\omega_0)$  is the index of refraction, and  $l$  is the cavity length excluding the crystal. Here we ignore other extra phase shifts that may occur at the surface of mirrors. Because of the degeneracy in the frequency, the double resonance is automatically satisfied.

On the other hand, because of the finite linewidth of each cavity mode, some other pairs of down-conversion fields with nondegenerate frequencies of  $\omega_{\pm m} = \omega_0 \pm m \Delta \Omega_{opo}$  may also satisfy the double resonance approximately to within the linewidth, with  $\Delta \Omega_{opo} = \pi c / L_{opo}$  as the frequency spacing between the longitudinal modes ( $L_{opo} = [l + n(\omega_0)d] / 2$  is the effective size of a standing-wave OPO cavity). The conditions for the double resonance of these nondegenerate mode are

$$\begin{aligned} & [l + n(\omega_0 + m \Delta \Omega_{opo})d] (\omega_0 + m \Delta \Omega_{opo}) \\ & = [2\pi(N_0 + m) + \delta_+] c, \\ & [l + n(\omega_0 - m \Delta \Omega_{opo})d] (\omega_0 - m \Delta \Omega_{opo}) \\ & = [2\pi(N_0 - m) + \delta_-] c, \end{aligned} \quad (11)$$

with  $m = 1, 2, \dots$  and  $|\delta_{+,-}| < \pi / \mathcal{F}$ . Here  $\pi / \mathcal{F}$  is the equivalent phase shift corresponding to the half linewidth of the cavity mode. So  $|\delta_{+,-}| < \pi / \mathcal{F}$  is the condition for resonance. The question is how large  $m$  is, which determines the number of modes that are in approximately double resonance. Obviously, we have

$$|\delta_+ \pm \delta_-| \leq |\delta_+| + |\delta_-| < 2\pi / \mathcal{F}. \quad (12)$$

This provides a constraint on  $m$ . Adding and subtracting Eq. (11) and using Eq. (12), we obtain

$$\Delta \Omega_{opo} < \sqrt{2\pi c / \mathcal{F} d |2n' + n'' \omega_0|} \quad (13)$$

and

$$m \approx (l + n_0 d + n' \omega_0 d) \Delta \Omega_{opo} / 2\pi c. \quad (14)$$

Here  $n_0 \equiv n(\omega_0)$ ,  $n' \equiv \partial n / \partial \omega$ , and  $n'' \equiv \partial^2 n / \partial \omega^2$ . Combining Eqs. (13) and (14), we have

$$m \leq \frac{(l + n_0 d + n' \omega_0 d)}{\sqrt{2\pi c \mathcal{F} |2n' + n'' \omega_0|}}. \quad (15)$$

For a crystal of KNbO<sub>3</sub> of 4 mm length and a monolithic standing-wave cavity, we have  $m \approx 26$ , i.e., about 20 pairs of down-conversion frequencies are on resonance with the cavity.

#### B. Type-II down-conversion

Two orthogonally polarized subharmonic fields are generated in type-II parametric down-conversion. Because of the birefringence in nonlinear crystals, indices of refraction for

the two fields are not same even at degenerate frequency. The condition for double resonance is even more restricted than the type-I case. Assuming we have double resonance at degenerate frequency

$$(l+n_1d)\omega_0=2\pi N_1c, (l+n_2d)\omega_0=2\pi N_2c \quad (16)$$

( $N_1 \neq N_2$ ), then the double resonance condition for the type-II case is

$$(l+n_1d)(\omega_0+\Delta\omega)=2\pi(N_1+\Delta N_1)c, \\ (l+n_2d)(\omega_0-\Delta\omega)=2\pi(N_2+\Delta N_2)c. \quad (17)$$

$N_{1,2}$  are integers and  $|\Delta N_1 - \Delta N_2| = 1, 2, 3, \dots$  so we have

$$\Delta\omega=2\pi c(\Delta N_1 - \Delta N_2)/(n_1 - n_2)d. \quad (18)$$

However, the type-II parametric down-conversion has a bandwidth of

$$\Delta\omega_{PDC} \approx \pi c/|n_1 - n_2|d, \quad (19)$$

derived from the phase-matching condition

$$|\Delta k|d = \frac{d}{c} |2\omega_0 n_0 - (\omega_0 + \Delta\omega)n_1 - (\omega_0 - \Delta\omega)n_2| \\ = \frac{d}{c} \Delta\omega |n_1 - n_2| \\ < \pi, \quad (20)$$

where we assume that phase matching is achieved at degenerate frequency ( $2n_0 = n_1 + n_2$ ). So  $\Delta\omega$  in Eq. (18) lies outside the bandwidth of down-conversion for nondegenerate frequency. We have double resonance only for degenerate frequency and thus achieve the single-mode operation in type-II down-conversion.

### C. Multimode OPO

In our experiment, the type-I scheme is used, so that there are numerous nondegenerate conjugate pairs of down-conversion on resonance together with the degenerate pair. These nondegenerate pairs will be located in the spectrum on the two sides of the degenerate pair with a spacing of  $\Delta\Omega_{opo}$ , the free spectral range of the OPO cavity, and have about the same strength as the degenerate one. For the nondegenerate modes, the conjugate pairs ( $\omega_{\pm m} = \omega_0 \pm m\Delta\Omega_{opo}$ ) are correlated and related by [28]

$$a_{out}(\omega_m + \omega) = G_1(\omega)a_{in}(\omega_m + \omega) + g_1(\omega)a_{in}^\dagger(\omega - m - \omega) \\ + G_2(\omega)b_{in}(\omega_m + \omega) + g_2(\omega)b_{in}^\dagger(\omega - m - \omega). \quad (21)$$

So the correlation in OPO is pairwise and the pairs are only connected through the pump field and are basically independent of each other.

### D. Filtered OPO

The existence of the nondegenerate modes of the OPO will not influence the homodyne detection in amplitude measurement because the beat frequency is usually larger than the electronic bandwidth of the detector and is filtered out electronically. For photons counting, however, all photon arriving in the detectors will produce a count indiscriminately. Thus we must eliminate the nondegenerate modes by filtering. In the absence of the intracavity frequency-selective elements, a passive filter such as Fabry-Pérot cavity is needed to get rid of the longitudinal modes. Transverse modes usually have a different frequency so that they are eliminated automatically if the cavity is tuned to the main TEM<sub>00</sub> mode. With the filter cavity, however, the spectrum will be altered and so will the correlation properties. The output field through the filter is given as [26]

$$c_{out}(\omega_0 + \omega) = R(\omega)c_{in}(\omega_0 + \omega) + T(\omega)d_{in}(\omega_0 + \omega), \quad (22)$$

with

$$R(\omega) = \frac{\kappa_1 - \kappa_2 + 2i\omega}{\kappa_1 + \kappa_2 - 2i\omega}, \quad T(\omega) = \frac{2\sqrt{\kappa_1\kappa_2}}{\kappa_1 + \kappa_2 - 2i\omega}. \quad (23)$$

Here  $\kappa_1$  and  $\kappa_2$  describe the decay rates for the mirrors of the filter cavity. With the boundary condition  $d_{in} = a_{out}$  and the assumption that  $c_{in}$  is in the vacuum field, we can calculate the spectrum of the field going through the filter cavity as

$$S_{FC}(\omega) = |T(\omega)|^2 [ |g_1(\omega)|^2 + |g_2(\omega)|^2 ] \\ = \frac{4\kappa_1\kappa_2}{(\kappa_1 + \kappa_2)^2 + 4\omega^2} \frac{16|\epsilon|^2\gamma_1(\gamma_1 + \gamma_2)}{[(\gamma_1 + \gamma_2)^2 + 4\omega^2]^2}, \quad (24)$$

where  $\gamma_1 + \gamma_2$  and  $\kappa_1 + \kappa_2$  are the bandwidths of the OPO cavity and the filter cavity, respectively. From the spectrum function of Eq. (24) we see that the bandwidth of the fields is narrowed further. If the bandwidth of the filter cavity is much smaller than that of the OPO cavity, i.e.,  $\gamma_1 + \gamma_2 \gg \kappa_1 + \kappa_2$ , then the total bandwidth will be mainly determined by the bandwidth of the filter cavity. On the other hand, if the bandwidth of the filter cavity is much larger than that of the OPO cavity, the filter cavity just seems as if it were not there. As for the correlation function between the fields, we will see later that it is also changed.

## IV. DISTRIBUTION OF THE TIME INTERVAL BETWEEN THE TWO DOWN-CONVERTED PHOTONS

### A. Ideal single-mode case

One of the quantities to characterize the two-photon state is the correlation time between the two down-converted photons. Attempts were made to measure it, but only the upper limit was given because the detectors available are not able to resolve the extremely short correlation time [1,2]. It was shown [3] that the correlation time is inversely proportional to the bandwidth of the detected down-converted fields. This

was indirectly confirmed by the interference method [17] and the autocorrelation method [29]. With the bandwidth significantly narrowed in an OPO, we should be able to resolve the correlation and make a direct measurement. Let us first calculate the correlation time from the theory of OPO for the single-mode case.

To find the correlation time between the two down-converted photons, we calculate the intensity correlation function defined as

$$\Gamma^{(2,2)}(\tau) = \langle \hat{E}^{(-)}(t) \hat{E}^{(-)}(t+\tau) \hat{E}^{(+)}(t+\tau) \hat{E}^{(+)}(t) \rangle. \quad (25)$$

From Eqs. (1), (2), (6), and (25) with some calculation, we find that

$$\begin{aligned} \Gamma^{(2,2)}(\tau) &= \frac{1}{(2\pi)^2} \left| \int [G_1(\omega)g_1(\omega) \right. \\ &\quad \left. + G_2(\omega)g_2(\omega)] e^{-i\omega\tau} d\omega \right|^2 \\ &= |\epsilon|^2 (\mathcal{F}/\mathcal{F}_0)^2 e^{-|\tau|(\gamma_1 + \gamma_2)}, \end{aligned} \quad (26)$$

where we dropped terms of higher order of  $|\epsilon|^2$  in Eq. (26) because  $|\epsilon| \ll \gamma_1 + \gamma_2$ . Note that from Eq. (25), the overall coincidence rate is calculated as

$$R_c = \int_{-\infty}^{\infty} \Gamma^{(2,2)}(\tau) d\tau = R_{cavity} \frac{\mathcal{F}}{\mathcal{F}_0}, \quad (27)$$

with  $R_{cavity}$  given from Eq. (7). If there were no loss, we would have  $R_c = R_{cavity}$ , i.e., the two-photon rate is exactly

the same as the single-photon rate, which is the signature of a two-photon state. The loss reduces the photon pairs by  $\mathcal{F}/\mathcal{F}_0$ . But we still have  $R_c \propto R_{cavity}$ , not  $R_{cavity}^2$ , which is for accidental coincidence rate. If we define the correlation time  $T_c$  between the two photons as the FWHH of the distribution in Eq. (26), then  $T_c$  is given as

$$T_c = 1.39/(\gamma_1 + \gamma_2) = 1.39/\Delta\omega_{opo}. \quad (28)$$

So, exactly the same as the single-pass case [3], the correlation time in the active filtering scheme is inversely proportional to the bandwidth of down-conversion.

## B. Multimode case

The above analysis is for a single-mode OPO. In the multimode situation, there are a number of modes separated by the free spectral range  $\Delta\Omega_{opo}$  of the OPO cavity. Assume  $2N+1$  of them exist, so the bandwidth of the fields is of the order of  $2N\Delta\Omega_{opo}$ . In our experiment  $\Delta\Omega_{opo}$  is about  $10^{10}$  Hz and  $N$  is about 10, so the bandwidth is of the order  $10^{11}$  Hz which is much larger than the bandwidth of the detectors ( $10^9$  Hz), and the correlation time is too small to resolve. What is measured will be an average over the detection time and the time interval distribution would simply be that of the electronic response function of the detection system as in Ref. [2] (see also Fig. 5 for a wide band source). However, as will be seen in Sec. V, the distribution is very much similar to the single-mode case in Eq. (26).

To understand this, let us calculate the correlation function for the multimode case, assuming  $N$  pairs of nondegenerate modes plus the degenerate mode. Similar to Eq. (26), we have

$$\begin{aligned} \Gamma_{mul}^{(2,2)}(\tau) &= \frac{1}{(2\pi)^2} \left| \sum_{m=-N}^N \int d\omega [G_1(\omega + m\Delta\Omega_{opo})g_1(\omega + m\Delta\Omega_{opo}) \right. \\ &\quad \left. + G_2(\omega + m\Delta\Omega_{opo})g_2(\omega + m\Delta\Omega_{opo})] e^{-i(\omega + m\Delta\Omega_{opo})\tau} \right|^2 \\ &= \Gamma_{single}^{(2,2)}(\tau) \left| \sum_{m=-N}^N e^{im\Delta\Omega_{opo}\tau} \right|^2 \\ &= \Gamma_{single}^{(2,2)}(\tau) \left| \frac{\sin(2N+1)\Delta\Omega_{opo}\tau/2}{\sin(\Delta\Omega_{opo}\tau/2)} \right|^2, \end{aligned} \quad (29)$$

where  $\Gamma_{single}^{(2,2)}(\tau)$  is the intensity correlation function of the single mode given in Eq. (26). As expected, the correlation function is zero if  $(2N+1)\Delta\Omega_{opo}\tau \sim 1$  and the correlation time is of order  $\tau_c \sim 1/(2N+1)\Delta\Omega_{opo}$ . However, the correlation function will revive at  $\Delta\Omega_{opo}\tau = 2M\pi$  ( $M=1,2,\dots$ ), but eventually will vanish at  $T_c$ . The revival of the correlation function is due to the discrete nature of the spectrum. The revival time  $\tau_r$  ( $=2\pi/\Delta\Omega_{opo} \sim 10^{-10}$  s) as well as the correlation time  $\tau_c$  is much shorter than the resolving time of

the detectors. Therefore, we will not be able to observe this phenomenon. But it will be reflected in the observed correlation function which is an average of Eq. (29) over the resolving time  $T_R$  of the detectors,

$$\Gamma_{obs}^{(2,2)}(\tau) = \frac{1}{T_R} \int_{\tau-T_R/2}^{\tau+T_R/2} \Gamma_{mul}^{(2,2)}(\tau') d\tau'. \quad (30)$$

On the one hand, because  $T_c \gg T_R$ ,  $\Gamma_{single}^{(2,2)}(\tau')$  is approxi-

mately equal to  $\Gamma_{single}^{(2,2)}(\tau)$  in Eq. (30) and can be taken outside the integral. On the other hand, because  $T_R \gg 1/\Delta\Omega_{opo}$ , the integral will average out the terms with  $e^{im\Delta\Omega_{opo}\tau'}$  after the expansion of the absolute value in Eq. (29). Hence we have

$$\Gamma_{obs}^{(2,2)}(\tau) = (2N+1)\Gamma_{single}^{(2,2)}(\tau). \quad (31)$$

So in the multimode case, the measured time interval distribution is not the response of the detection system but has exactly the same form as that of the single-mode case, and is  $2N+1$  times larger.

### C. Filtered case

With a passive cavity to filter the non-degenerate modes, the degenerate mode is also modified. From Eqs. (6), (23), and (25) with some calculation, we can find that

$$\Gamma_{filtered}^{(2,2)}(\tau) \propto \left| \frac{e^{-\tau\Delta\omega_{C2}/2}}{\Delta\omega_{C2}} - \frac{e^{-\tau\Delta\omega_{opo}/2}}{\Delta\omega_{opo}} \right|^2, \quad (32)$$

where  $\Delta\omega_{C2} = \kappa_1 + \kappa_2$  and  $\Delta\omega_{opo} = \gamma_1 + \gamma_2$  are the bandwidths of the filter and OPO cavities, respectively. With the filter cavity, the relationship between the correlation time and the bandwidth of the output field is no longer a simple relationship of inverse proportion, but a complex one. For the following two extreme cases we can make a good approximation and obtain simpler relations between the bandwidth and the correlation time.

$$(1) \kappa_1 + \kappa_2 \gg \gamma_1 + \gamma_2,$$

$$T_c = 1.39/(\gamma_1 + \gamma_2) = 1.39/\Delta\omega_{opo}. \quad (33)$$

In this case, the effect of the filter cavity is just to eliminate those nondegenerate longitudinal modes, but do nothing for the degenerate mode. The effective bandwidth is not altered by such a filter. We have the single-mode case.

$$(2) \kappa_1 + \kappa_2 \ll \gamma_1 + \gamma_2,$$

$$T_c = 2 \ln 2 / (\kappa_1 + \kappa_2) = 1.39/\Delta\omega_{C2}. \quad (34)$$

In this case, the filter cavity not only eliminates the longitudinal modes, but also cuts the effective bandwidth to that of its own. Such a filter has a significant effect on the correlation time, which is again inversely proportional to the bandwidth of the detected fields.

## V. EXPERIMENT

The schematic diagram of the experiment is shown in Fig. 1. An Ar-ion-laser-pumped single-mode cw Ti:sapphire laser operating at around 855 nm is the primary source for the experiment. A 5-mm-long  $\text{KbNO}_3$  crystal is placed at the waist inside the laser for intracavity frequency doubling. The harmonic field at 427 nm from the frequency doubling interacts with the OPO cavity for frequency down-conversion. It has a typical power of 5 mW and is mode matched to an auxiliary cavity C1. The semimonolithic OPO cavity C0 consists of a flat mirror (M) and a 4-mm-long  $\text{KbNO}_3$  crystal polished at one end with a 7-mm curvature and at the other

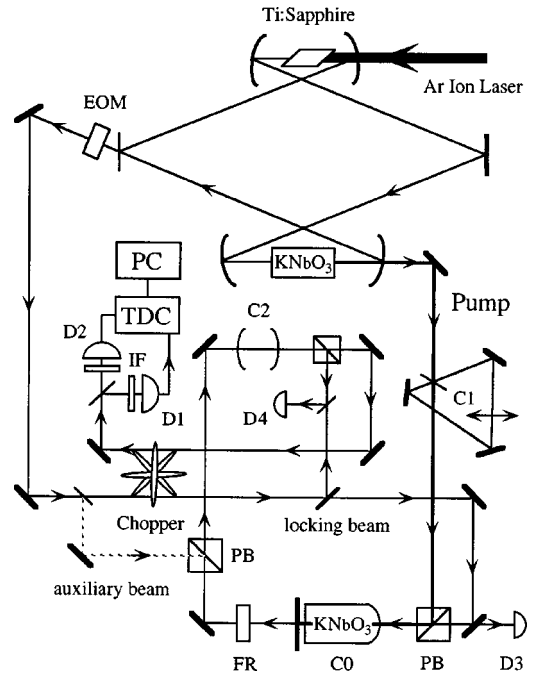


FIG. 1. Schematic diagram of the experiment setup. EOM: electro-optic phase modulator for the rf sideband creation; IF: interference filter; D1, D2: avalanche photodetectors (APD); TDC: time-to-digital converter; D3, D4: fast photodetectors for cavity locking; PB: polarization beamsplitter; FR: Faraday rotator for isolation; C0: OPO cavity; C1: mode matching cavity for the pump field; C2: filter cavity.

end with a flat surface. The curved side is optically coated so that it is highly reflective at 855 nm ( $R > 99.99\%$ ). The flat face is antireflection coated for both 855 and 427 nm. The flat output mirror M has a measured transmissivity of 1.5% at 855 nm and is placed closely (with a 0.5-mm gap) to the flat side of the crystal. The flat mirror is mounted on a piezoelectric transducer so that the OPO cavity length can be controlled electronically for tuning onto resonance with the laser frequency. Such a compact design is intended for an optimum bandwidth of down-conversion taking into consideration both signal level and bandwidth as well as the stability of the OPO system. Both the curved side of the crystal and the flat output coupler have a relatively high transmission ( $T > 80\%$ ) for 427 nm so that the pump field interacts only once with the nonlinear medium. This eliminates complications involved in resonating the cavity at two wavelengths (855 nm and 427 nm). However, this creates a problem for the mode match of the pump field to the  $\text{TEM}_{00}$  mode of the OPO cavity. Such a mode match is important not only because it can increase the pump efficiency but also because it can inhibit the excitation of the complicated transverse spatial modes of the OPO. The mode match is done by matching both the harmonic pump field from the laser and the harmonic field from the OPO cavity to the auxiliary cavity C1, simultaneously. To generate the harmonic field from the OPO cavity, we inject into the cavity for frequency doubling (the reverse process of down-conversion) with an auxiliary beam that is a small portion of the laser output [30].

The theory presented earlier is for a single-mode OPO

resonant at degenerate frequency. In the experiment, because the two down-converted fields have the same polarization in the type-I scheme, there are numerous nondegenerate conjugate pairs of down-conversion on resonance simultaneously with the degenerate pair. The nondegenerate pairs ( $\omega_0 \pm m\Delta\Omega_{opo}$ ,  $m$  is an integer) will be located in the spectrum on the two sides of the degenerate pair ( $\omega_0$ ) with a spacing of  $\Delta\Omega_{opo}$ , the free spectral range of the OPO cavity, and have about the same strength as the degenerate one. So a passive filter is needed to further eliminate them. This is done with another cavity  $C2$  which has a bandwidth larger than that of the single-mode down-conversion. The resonance condition is achieved by locking  $C0$  and  $C2$  to the laser frequency (which is also the degenerate frequency  $\omega_0$  of the down-conversion) by the Pond-Drever rf sideband method [31] via photodiodes  $D3$ ,  $D4$  with partitioned beams from the auxiliary laser beam. These beams are also used to align and mode-match  $C0$  to  $C2$ . However, the locking beam has the same frequency and polarization as the down-converted signal field, creating an enormous background. To eliminate the background, we alternate the periods of cavity locking and signal detection with a mechanical chopper. Because of the rigid and compact structure of  $C0$  and  $C2$ , the cavities remain locked even in the period when the locking beam is blocked for signal detection. In the following, we will describe some experiments based on the setup above.

#### A. Enhancement effect by cavity resonance

First, we examine the enhancement of parametric down-conversion due to cavity resonance. In this experiment, we will compare the signal levels in two situations: one with cavity and the other without cavity. To make an accurate measurement of the signal, we place the detectors directly at the output of the OPO without going through the filter cavity  $C2$ . Interference filters are needed in front of the detectors [avalanche photodiodes (APD)  $D1$ ,  $D2$ , EG&G SPCM-AQ-121] to eliminate background light mainly from the pump field.

For the situation with an enhancement cavity for down-conversion, we register the count rate as well as the coincidence rate as a function of the cavity length of  $C0$ , as shown in Fig. 2. A strong resonance effect is obvious. It should be noted that at the middle between the degenerate  $\omega_0$  peaks, there is an extra resonance peak for  $\omega_0 \pm \Delta\omega_{opo}/2$ , so that there are two peaks in one free spectral range of the OPO cavity. At the highest peak, we obtain the calibrated count rate  $R_{resonance} = 1.6 \times 10^7/\text{sec}$  at 1-mW pumping. The smaller side peaks are higher-order transverse cavity modes excited by the imperfectly mode-matched pump. Their effect is to have a smaller main peak than the case with perfect mode matching. The two-photon nature of the source is evidenced in the linear plot of the count rate against the coincidence rate (Fig. 3). The finesse of the OPO cavity is measured to be  $\mathcal{F}_{opo} = 350$  and the free spectral range of the OPO cavity is calculated as  $\Delta\Omega_{opo} = 9.80 \times 10^{10}$  rad/sec from the effective cavity length of  $L_{opo} = 9.6$  mm. So the bandwidth of the OPO cavity is  $\Delta\omega_{opo} = \Delta\Omega_{opo}/\mathcal{F}_{opo} = 2.8 \times 10^8$  rad/sec. However, as we discussed in Sec. III, without

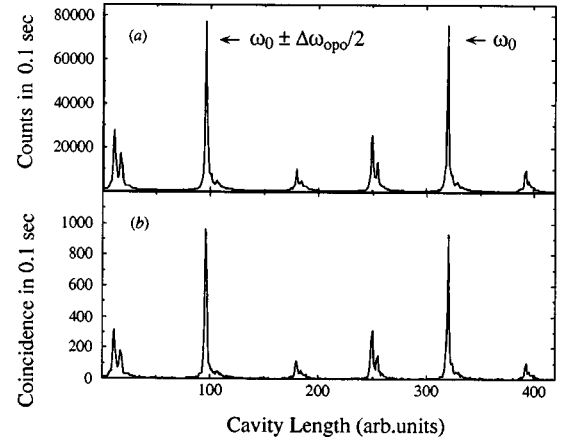


FIG. 2. Single-photon and coincidence counting rates as a function of the length of OPO cavity. The scan is over one free spectral range.

the filter cavity  $C2$  this type of OPO will produce multiple longitudinal modes with  $\Delta\Omega_{opo}$  as the separation between the modes. The number of modes that arrive at the detectors is determined by the ratio of the bandwidth  $\Delta\omega_{IF}$  of the interference filter (see below) to mode spacing  $\Delta\Omega_{opo}$  as  $N = 13$  (see also later in the mode structure). The signal rate for the single mode is then  $R_{cavity} = R_{resonance}/N = 1.2 \times 10^6/\text{sec}$ .

For the single-pass case, we measure the count rate with the output coupler removed. The calibrated result is  $R_{singlepass} = 10^5/\text{sec}$  at 1 mW. The bandwidth in this case is determined by that of the interference filter, which is  $\Delta\omega_{IF} = 1.29 \times 10^{12}$  rad/sec ( $\Delta\lambda = 0.5$  nm). Hence, the measured enhancement factor is  $B_{exp} = 5.5 \times 10^4$ . The theoretical prediction from Eq. (9) gives  $B_{th} = 5.1 \times 10^4$  for the measured values of  $\mathcal{F} = 350$  and  $\mathcal{F}_0 = 420$ , which agrees relatively well with the experimental result. The discrepancy may arise from the inaccurate measurement of cavity finesse, which will also give rise to a less accurate estimate of the down-conversion bandwidth. The crude model for the single-pass case may also contribute to the problem.

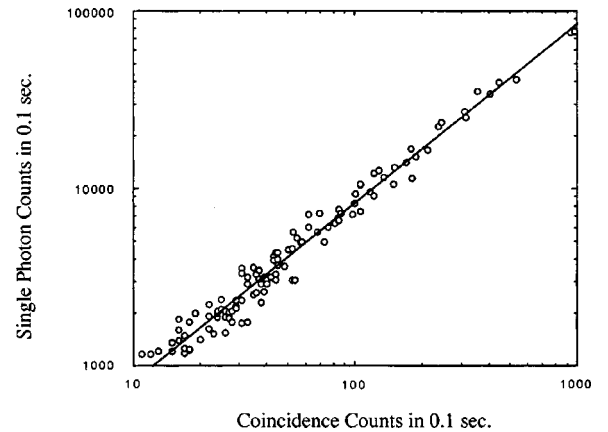


FIG. 3. Single-photon rate vs coincidence rate from the data in Fig. 2. The solid curve is a linear fit with a slope of 1.01 in log-log scale.

### B. Spectrum and mode structure

Because of the type-I scheme of parametric down-conversion, there are many pairs of nondegenerate modes simultaneously on resonance, producing about the same strength as the degenerate one. For the single-mode operation, we use the filter cavity  $C2$  to eliminate the nondegenerate modes. However, to ensure that the center frequency of the filter coincides with the degenerate mode, we need to check the spectrum of the OPO. This is done by scanning the filter cavity  $C2$ . On the one hand, in order to have a faithful measurement, the free spectral range (FSR) of  $C2$  is normally wider than the full range of the OPO modes. This means that the cavity size of  $C2$  must be much shorter than that of the OPO cavity, which is already very short. On the other hand, the role of the cavity  $C2$  is to filter out the nondegenerate modes and let the degenerate mode pass. So it is only necessary to set the bandwidth of  $C2$  wider than that of the single mode of OPO. In the experiment, the initial size of the standing-wave filter cavity is 3.35 mm, and the measured finesse of the cavity is 400, which gives the FSR of  $C2$  as  $\Delta\Omega_{C2} = \pi c/L_{C2} = 2.81 \times 10^{11}$  rad/sec and the bandwidth of  $C2$  as  $\Delta\omega_{C2} = 7.02 \times 10^8$  rad/sec  $>$   $\Delta\omega_{opo} = 2.8 \times 10^8$  rad/sec. As will be seen later, the size of the cavity  $C2$  is varied to change the passing bandwidth of the cavity. Because the range of the discrete longitudinal modes of the OPO is many times of the FSR of the filter cavity  $\Delta\Omega_{C2}$ , we expect them to appear in one FSR with a different order number. In the experiment, we lock the OPO cavity to the laser frequency and scan continuously the filter cavity length over around one free spectral range of the filter cavity. Figure 4(a) shows a typical result from such a scan.

We can see that there are about 32 peaks in one FSR of the filter cavity in Fig. 4(a). But because the FSR of the  $C2$  is not much larger than the range of the whole spectrum, this does not mean that there are 32 modes from OPO. In the following, we will make a simulation of the outcome from the filter cavity  $C2$  for the spectrum of OPO based on the known sizes of the two cavities and compare it to the experimental result of Fig. 4(a). In the experiment, the actual size of the filter cavity is 3.35 mm, while the effective length of OPO is estimated as 9.6 mm. So we have the free spectral range for the filter cavity and mode spacing for OPO longitudinal modes:

$$\begin{aligned}\Delta\Omega_{opo} &= \pi c/L_{opo} = 9.8 \times 10^{10}, \\ \Delta\Omega_{C2} &= \pi c/L_{C2} = 2.81 \times 10^{11}.\end{aligned}\quad (35)$$

Because  $\Delta\Omega_{C2}/\Delta\Omega_{opo} \approx 2.9$ , only three OPO modes ( $\omega_0$ ,  $\omega_0 + \Delta\Omega_{opo}$ ,  $\omega_0 + 2\Delta\Omega_{opo}$ ) will appear in one FSR of the filter cavity if we only allow one order number. And if we start with the degenerate mode of  $\omega_0$ , the other two will increase by an equal step. All the other modes with higher frequency will appear outside the FSR of the filter cavity for the same order number. But if we allow a different order number to appear as in experiment, the modes outside the FSR will show up inside the FSR with a lesser order number of  $k = \text{int}(m\Delta\Omega_{opo}/\Delta\Omega_{C2})$  than the degenerate mode, where ‘int’ is the integer function that takes the integer part of a

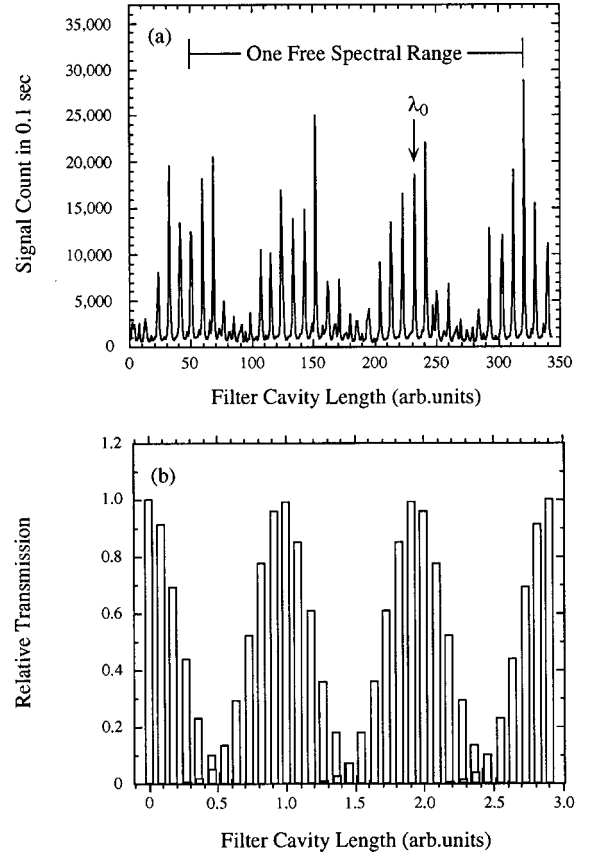


FIG. 4. (a) The spectrum of OPO output in one free spectral range of the filter cavity  $C2$ . The degenerate frequency (laser frequency) is marked with an arrow. (b) Simulation of the spectrum of OPO in one FSR of  $C2$ .

number. So its position in the FSR will be  $m\Delta\Omega_{opo} - k\Delta\Omega_{C2}$ . The strength of this mode is calculated by a Gaussian profile centered at the degenerate frequency,

$$f(\omega_0 + m\Delta\Omega_{opo}) = \exp[-(m\Delta\Omega_{opo})^2/2\sigma^2], \quad (36)$$

where the width  $\sigma$  is obtained from the bandwidth  $\Delta\omega_{IF}$  of the interference filter placed in front of the detector. We can likewise find the position and strength of the mode with frequency less than  $\omega_0$ . Figure 4(b) shows the result of the simulation. The structure coincides with that of Fig. 4(a), indicating that we have a correct understanding of the OPO mode structure. It should be noted that the irregular size of the peaks in Fig. 4(a) is caused by unstable locking of the OPO cavity and does not reflect the true height of the modes.

### C. Time interval distribution: Single mode and multimode

As the last part of the experiment, we examine the correlation property of the two down-converted photons by directly measuring the distribution of the time interval between the arrivals of the two photons. Since the two photons are degenerate in both frequency and polarization, it is impossible to separate them completely. So we will use a beam splitter to divide half of the photon pairs while the other half will not be separated, and we lose 50% of the coincidence.

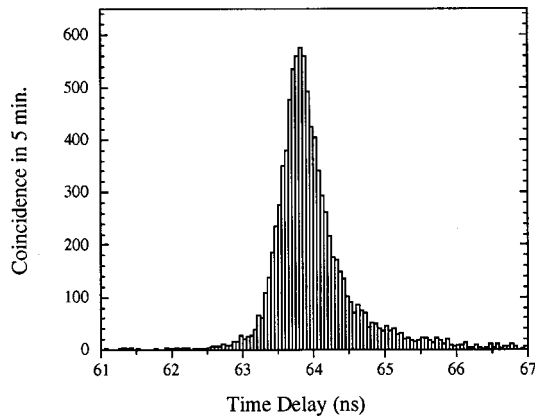


FIG. 5. Electronic response of the detection system to a two-photon source with extremely short correlation time ( $<1$  ps).

The two outputs from the beam splitter are detected by two APD detectors, which generate two electric pulses for input to a time-to-digital converter (TDC, Lecroy 2228A). The TDC measures the time difference between the arrivals of the two photons. The resolution of the TDC is 50 ps. However, the average resolution time of the APDs is about 0.5 ns, which is measured from the distribution in Fig. 5 with a wide-band source of parametric down-conversion. (This is done by taking out the output coupler  $M$  of the OPO and the source has an estimated correlation time as  $1/\Delta\Omega_{IF} \approx 1$  ps.) So we set the coincidence window for the TDC as 0.5 ns. We measure the coincidence as a function of the time interval. Figure 6 shows the result of the measurement without the filter cavity  $C2$ , which corresponds to the multimode case. The solid curve is a weighted  $\chi^2$  fit to Eq. (26) for the multimode case. The  $\chi^2$  is weighted on the measurement uncertainty. The value of the weighted  $\chi^2$  per degree of freedom is 1.13, which is close to the ideal value of one, indicating an excellent fit. To obtain the single mode correlation function, we use the filter cavity  $C2$  to delete the nondegenerate modes. We vary the length of the cavity in order to change the passing bandwidth accordingly. Figure 7(a)–7(c) show the distribution for three different lengths of the cavity: 3.35,

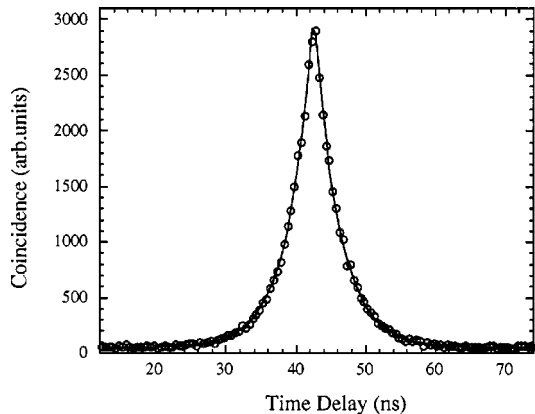


FIG. 6. Time interval distribution for multimode OPO output. The solid curve is a weighted  $\chi^2$  fit to Eq. (26). The average  $\chi^2$  per data point is 1.13.

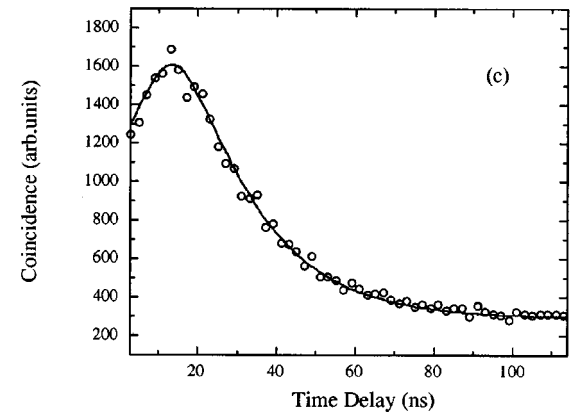
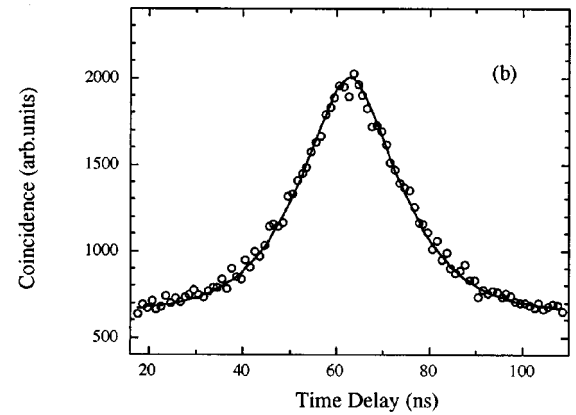
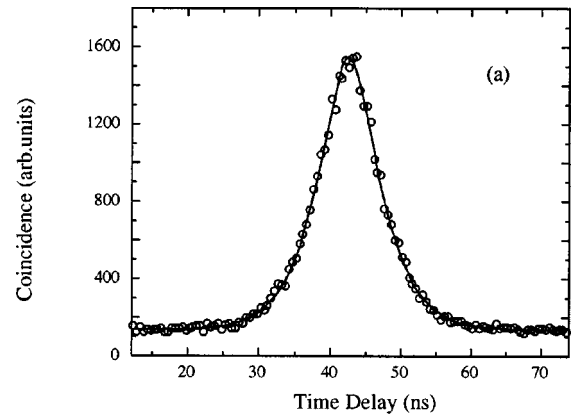


FIG. 7. Time interval distribution of filtered single-mode OPO output for various lengths of the filter cavity  $C2$ , (a) 3.35 mm, (b) 20.17 mm, (c) 41.50 mm. The solid curves are a weighted  $\chi^2$  fit to Eq. (32). The average  $\chi^2$  per data are (a) 1.04; (b) 1.14; (c) 1.00.

20.17, and 41.50 mm, respectively. The solid curves are a weighted  $\chi^2$  fit to Eq. (32). The values of the weighted  $\chi^2$  per degree of freedom are given in the figure caption. As seen, they are all close to one, indicating excellent fits. Because the distribution in Eq. (32) is not a trivial function and depends on two parameters, i.e., the bandwidths of OPO and the filter, it is not straightforward to define a correlation time. In order to fully test the model in Eq. (32), we plot in Fig. 8 the best fitted values of bandwidths for OPO and the filter cavities, which somewhat represent the inverse of the correlation time, against the directly measured values for all four distributions in Figs. 6 and 7. A relative good fit can be seen.

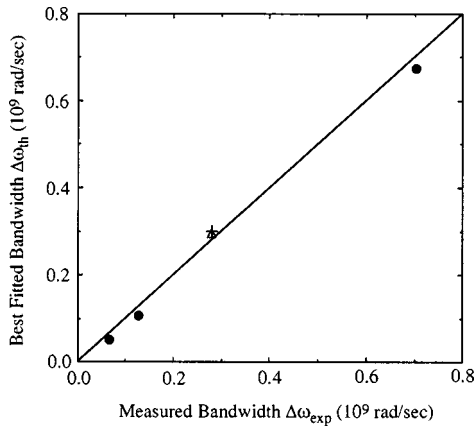


FIG. 8. Comparison of the best fitted parameters of  $\Delta\omega_{opt}$ ,  $\Delta\omega_{C2}$  vs experimentally measured values. The solid circles correspond to the filter cavity C2, the triangle is for OPO cavity from single-mode data of Fig. 7, and the cross is for the OPO cavity from the multimode data of Fig. 6.

The errors are mainly from the crude measurement of the finesse of the cavities.

## VI. CONCLUSION AND DISCUSSION

In this paper we have presented a successful implementation of an active filtering scheme for the generation of the narrow-band two-photon state. We have applied the quantum theory of the optical parametric oscillator to the regime far below threshold and have experimentally demonstrated that

the signal rate is significantly enhanced and the bandwidth is substantially reduced due to optical resonance. The enhancement factor per frequency mode is of the order of the square of the number of bounces of light before it goes outside the resonator. By operating the device far below threshold, we ensured the two-photon nature of the output state. The reduction in the down-conversion bandwidth allows us to directly measure the photon correlation function for the time interval distribution between the arrivals of the two photons. The excellent agreement between the experiment and the theory supports that the theory of OPO below threshold is applicable to the regime of far below threshold.

OPO with type-I phase matching produces two inseparable down-converted photons. To obtain the two-photon state with separated photons, we should use type-II phase-matching down-conversion because the two photons so produced have orthogonal polarization and can be separated by a polarization beam splitter. As we have seen in Sec. III, such a scheme will automatically achieve single-mode operation. But its implementation is harder than the type-I scheme because it involves simultaneous resonance of two polarized components. Nevertheless, a narrow-band two-photon source will enable us to perform a number of quantum interference experiments involving independent fields for quantum information processing.

## ACKNOWLEDGMENT

This work was supported by the Office of Naval Research.

- 
- [1] D. C. Burnham and D. L. Weinberg, Phys. Rev. Lett. **25**, 84 (1970).
  - [2] S. Friberg, C. K. Hong, and L. Mandel, Phys. Rev. Lett. **54**, 2011 (1985).
  - [3] C. K. Hong and L. Mandel, Phys. Rev. A **31**, 2409 (1985).
  - [4] Z. Y. Ou and L. Mandel, Phys. Rev. Lett. **61**, 50 (1988); Y. H. Shih and C. O. Alley, *ibid.* **61**, 2921 (1988).
  - [5] P. G. Kwiat, K. Mattle, H. Weinfurter, A. Zeilinger, A. V. Sergienko, and Y. H. Shih, Phys. Rev. Lett. **75**, 4337 (1995).
  - [6] R. Ghosh and L. Mandel, Phys. Rev. Lett. **59**, 1903 (1987); Z. Y. Ou and L. Mandel, *ibid.* **62**, 2941 (1989).
  - [7] J. Franson, Phys. Rev. Lett. **62**, 2205 (1989).
  - [8] D. V. Strekalov *et al.*, Phys. Rev. Lett. **74**, 3600 (1995).
  - [9] T. J. Herzog, P. G. Kwiat, H. Weinfurter, and A. Zeilinger, Phys. Rev. Lett. **75**, 3034 (1995).
  - [10] D. Bouwmeester, J-W. Pan, K. Mattle, M. Eibl, H. Weinfurter, and A. Zeilinger, Nature (London) **390**, 575 (1997).
  - [11] J-W. Pan, D. Bouwmeester, H. Weinfurter, and A. Zeilinger, Phys. Rev. Lett. **80**, 3891 (1998).
  - [12] D. Bouwmeester, J-W. Pan, M. Daniell, H. Weinfurter, and A. Zeilinger, Phys. Rev. Lett. **82**, 1345 (1999).
  - [13] L.-A. Wu, H. J. Kimble, J. L. Hall, and H. Wu, Phys. Rev. Lett. **57**, 2520 (1986).
  - [14] J. H. Shapiro and K.-X. Sun, J. Opt. Soc. Am. B **11**, 1130 (1994).
  - [15] G. Magyar and L. Mandel, Nature (London) **198**, 255 (1963).
  - [16] Z. Y. Ou, Phys. Rev. A **37**, 1607 (1988).
  - [17] C. K. Hong, Z. Y. Ou, and L. Mandel, Phys. Rev. Lett. **59**, 2044 (1987).
  - [18] J. G. Rarity and P. R. Tapster, in *Photons and Quantum Fluctuations*, edited by E. R. Pike and H. Walther (Adam Hilger, Bristol, 1989); J. Opt. Soc. Am. B **6**, 1221 (1989).
  - [19] J. G. Rarity, Ann. (N.Y.) Acad. Sci. **755**, 91 (1995); M. Zukowski, A. Zeilinger, and H. Weinfurter, *ibid.* **755**, 624 (1995).
  - [20] Z. Y. Ou, J.-K. Rhee, and L. J. Wang, Phys. Rev. A **60**, 593 (1999).
  - [21] See, for example, S. Haroche and D. Kleppner, Phys. Today **32(1)**, 24 (1989).
  - [22] A. Aiello, D. Fargion, and E. Cianci, Phys. Rev. A **58**, 2446 (1998).
  - [23] Z. Y. Ou and Y. J. Lu, Phys. Rev. Lett. **83**, 2556 (1999).
  - [24] R. L. Byer and S. E. Harris, Phys. Rev. **168**, 225 (1968).
  - [25] B. Yurke, Phys. Rev. A **29**, 408 (1984).
  - [26] M. J. Collett and C. W. Gardiner, Phys. Rev. A **30**, 1386 (1984).

- [27] A. Heidmann, R. J. Horowicz, S. Reynaud, E. Giacobino, C. Fabre, and G. Camy, *Phys. Rev. Lett.* **59**, 2555 (1987).
- [28] C. W. Gardiner and C. M. Savage, *Opt. Commun.* **50**, 173 (1984).
- [29] I. Abram *et al.*, *Phys. Rev. Lett.* **57**, 2516 (1986).
- [30] E. S. Polzik, J. Carri, and H. J. Kimble, *Phys. Rev. Lett.* **68**, 3020 (1992); *Appl. Phys. B: Photophys. Laser Chem.* **55**, 279 (1992).
- [31] R. W. Drever, J. L. Hall, F. V. Kowalski, J. Hough, G. M. Ford, A. J. Munley, and H. Ward, *Appl. Phys. B: Photophys. Laser Chem.* **31**, 97 (1983).